Carbohydrate Polymers 108 (2014) 65–74

Contents lists available at ScienceDirect

Carbohydrate Polymers

journal homepage: www.elsevier.com/locate/carbpol

Recycling of textile dye using double network polymer from sodium alginate and superabsorbent polymer

V. Dhanapal [a], K. Subramanian [b,*]

[a] Department of Physical Sciences, Bannari Amman Institute of Technology, Sathyamangalam, 638401 Erode Dt, Tamil Nadu, India
[b] Department of Biotechnology, Bannari Amman Institute of Technology, Sathyamangalam, 638401 Erode Dt, Tamil Nadu, India

ARTICLE INFO

Article history:
Received 7 January 2014
Received in revised form 18 February 2014
Accepted 5 March 2014
Available online 24 March 2014

Keywords:
Dye removal
FT-IR
Thermogravimetric analysis
Adsorption isotherm kinetics
Thermodynamics

ABSTRACT

Double network polymers (DNP) of different compositions were photosynthesized using sodium alginate (NaAlg) and superabsorbent polymer (SAP). They were characterized by FT-IR, thermal stability (TG), morphology by scanning electron microscopy (SEM), and its mechanical properties were also evaluated for their dye adsorption–desorption characteristics via adsorption isotherms at different temperature and pH values. The spectrophotometric determination of adsorbed dye indicated that the maximum dye uptake in column mode was 439 mg/g. The nearly identical visible absorption spectra of the fabrics dyed with virgin and recovered dyes indicated that the recovered dye retained its structural stability during column recovery and the dyed fabrics possess good color fastness properties. Dye adsorption kinetic and de-sorption mechanism were found to be pseudo-first-order and non-Fickian, respectively. The adsorption showed best fit for Langmuir adsorption isotherm. The changes in the thermodynamic parameters namely Gibbs free energy (ΔG°), entropy (ΔS°) and enthalpy (ΔH°) for the dye-adsorbent systems inferred that the adsorption process was spontaneous and exothermic.

1. Introduction

Industrial effluents are discharged into land and water from industries such as dying, paper, plastic, leather, food and mineral processing (Orthman, Zhu, & Lu, 2003) without proper treatment leading to complex environmental pollution and health problems. Textile dying process generates huge quantity of toxic effluents which contains unabsorbed residual dyes and salts that spoils the environment enormously. Low biochemical oxygen demand and high chemical oxygen demand (Nasr, Abo El-Ola, Ramadan, & Hashem, 2006) are the characteristics of dye effluent. Many synthetic organic dyes from effluent are highly toxic and endanger the aquatic life and environment (Kadirvelu, Brasquet, & Cloiree, 2000). The reactive dyes may be mutagenic and carcinogenic (Rajeswari, Namasivayam, & Kadirvelu, 2001) and can cause severe damage to the liver, digestive and the central nervous system of human beings and affect agricultural cultivation and underground water. Hence there is an urgent necessity to remove dyes from the effluent before being discharged into land and water using appropriate physico-chemical methods. Among them the adsorption technology which employs activated carbon (Nasr et al., 2006), natural clays (Tahir & Rauf, 2006), modified clays (Baskaralingam, Pulikesi, Ramamurthi, & Sivanesan, 2006), fly ash (Dhodapkar, Rao, Pande, & Kaul, 2006), etc. as adsorbents is generally considered to be a cost effective method to bring down the concentration of unabsorbed dyes in dye effluent (Tsai, Chang, Ing, & Chang, 2004). In recent years SAPs (Paulino et al., 2006) are progressively being used to remove the colors, toxic and heavy metal substances and other pollutants from waste water through adsorption mechanism which involves mass transfer from the liquid phase to the adsorbent and subsequent binding via physico-chemical interaction (Wang & Liu, 2013; Zheng, Huang, & Wang, 2011).

SAPs are physico-chemically crosslinked three-dimensional networks of hydrophilic polymer chains with properties between liquids and solids. These polymers can imbibe and retain large amount of water and water soluble substances without dissolving and losing their structural integrity (Guilherme et al., 2005). Due to these properties, they are finding widespread applications (Dhanapal, Vijayakumar, & Subramanian, 2013) in bioengineering, biomedicine, agriculture, water purification, separation process, effluent treatment, etc. For constant use, the mechanical strength of these polymers must be good enough to withstand varies shearing forces. But unfortunately these polymers are not having enough mechanical properties for the continuous applications. It has been

* Corresponding author. Department of Biotechnology, Bannari Amman Institute of Technology, Sathyamangalam- 638 401 Erode Dt, Tamil Nadu, India,
Cell: +91 9894372411; Tel.: +91 4295 226254, fax: +91 4295 226666.
E-mail addresses: drksubramanian@rediffmail.com, dhanapalv@bitsathy.ac.in (K. Subramanian).

http://dx.doi.org/10.1016/j.carbpol.2014.03.013
0144-8617/

reported (Guilherme et al., 2005) that the mechanical properties of SAPs can be improved by double network formation through physico-chemical crosslinking in the presence of another pre-formed polymer (Gong, Katsuyama, Kurokawa, & Osada, 2003). In this laboratory SAPs are synthesized for water conservation in agricultural applications and effluent water treatment, but their mechanical properties are not good for broader applications. Hence an attempt is made to widen its application by improving its mechanical properties by double network formation taking NaAlg as the second pre-formed polymer. The primary choice of NaAlg for double network formation is due to the attractive combination of availability, price, and its performance in effluent water treatment. Besides these it possesses good water solubility, non-toxicity, biodegradability and biocompatibility (Nakajima et al., 2009).

DNPs were reported (Marandi, Sharifnia, & Hosseinzadeh, 2006) to be good candidate matrix for the removal of dye from the textile effluent. This was done by photo crosslinking of SAP and $CaSO_4$ induced ionic crosslinked NaAlg using 254 nm radiations. NaAlg, a natural ionic hydrophilic linear polysaccharide containing β-D-mannuronic acid and α-L-guluronic acid with —OH and —COO^- groups is commonly used in the synthesis of tough hydrogels for different applications (Guilherme et al., 2005). The sugar residues in NaAlg can either be arranged in blocks or they can be randomly distributed. Moreover, NaAlg grafted/crosslinked SAP was shown to be an excellent adsorbent for the removal of colored materials and toxic heavy metal ions from industrial effluent (Kobaslija & McQuade, 2006), Hence the present investigation involves the synthesis of a potential DNP by photo crosslinking of NaAlg on reported SAP (Dhanapal et al., 2013) and its subsequent evaluation as an adsorbent to remove the dyes from the textile dye effluent.

2. Experimental

2.1. Materials

Acrylic acid (AA, Himedia, Mumbai) and potassium persulphate (KPS, NICE, Cochin) were used after purification by vacuum distillation (700 mm Hg) and recrystallization with double distilled water, respectively. NaAlg, calcium sulphate ($CaSO_4$), trimethylolpropane triacrylate (TMPTA) (Himedia, Mumbai), N-isopropyl acrylamide (NIPAAm, Aldrich), acetone, methanol, isopropanol, potassium hydroxide (Rankem, New Delhi), sodium chloride (NaCl), sodium carbonate (Na_2CO_3) (Merck), reactive blue 4 (RB 4) (Sigma–Aldrich, molecular weight = 637.43, color index no = 61205, λ_{max} = 595 nm) were used as received, and the chemical structure of RB 4 is shown in Fig. 1(a).

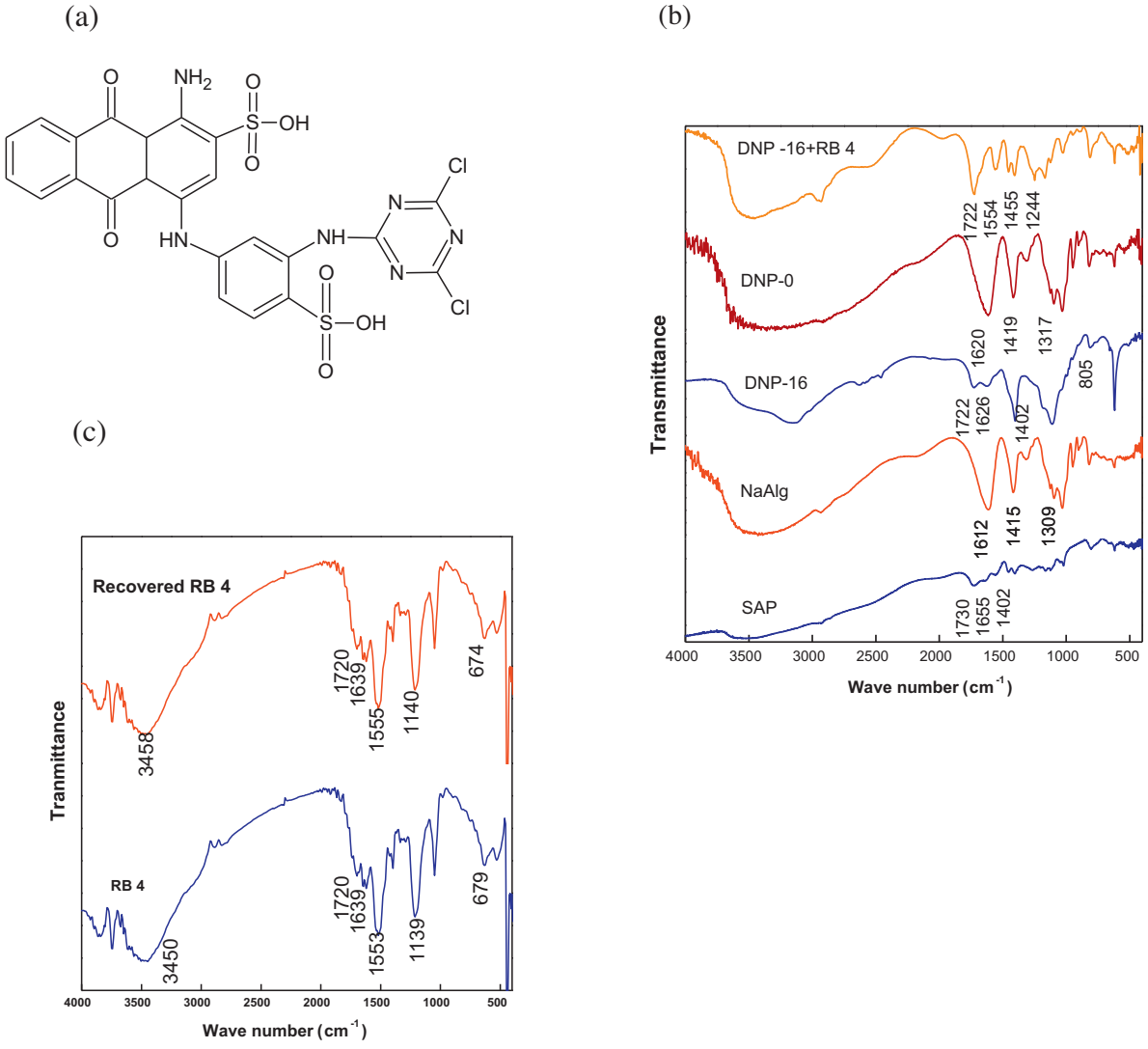

Fig. 1. Chemical structure of RB 4 (a), FT-IR spectra of SAP (b), NaAlg (b), DNP-16 (b), DNP-0, DNP-16 + RB 4 (b) and virgin and recovered RB 4 (c).

2.2. Synthesis of SAP

SAPs were prepared by free radical copolymerization of AA, NIPAAm and TMPTA using KPS initiator in aqueous solution (40 mL) as reported (Dhanapal et al., 2013).

2.3. Ionic crosslinking of NaAlg

SAP (1st network) was allowed to equilibrium swelling in an aqueous solution containing dissolved NaAlg. $CaSO_4$ slurry in water was added to the reaction mixture at 30 °C and thoroughly stirred to form ionic crosslinks between NaAlg and SAP.

2.4. Photo crosslinking of NaAlg and chemically crosslinked SAP

For photo crosslinking, an aqueous solution containing the ionically crosslinked NaAlg and SAP were taken in a 100 mL beaker and nitrogen purged for 20 min to remove the dissolved oxygen. This was then irradiated with UV light (10 W, 254 nm) for the durations of 0, 6, 12, 18, 24, 30 h by keeping the distance between the lamp and solution surface in the beaker as 15 cm. The second network, ionically crosslinked alginate was subsequently photo crosslinked onto the first network (Yasuda et al., 2005). The obtained gel was washed by immersing in fresh distilled water twice per day over a period of 1 week to remove any unreacted materials and then dried in hot air oven at 60 °C for 24 h. The dry polymer was powdered, sieved (mesh size 100 and 150 μm) and stored after vacuum drying.

2.5. Chemical characterization of photo crosslinked NaAlg-SAP

FT-IR spectra of NaAlg photo crosslinked SAP, virgin and recovered RB 4 were recorded in KBr pellet for the spectral range 400–4000 cm^{-1} using Shimadzu FT-IR-8400S by accumulating 48 scans at a resolution of 2 cm^{-1}. Thermal degradation (TG/DTG) studies were performed on TGA Q 500 V20.10 Build 36 with a sample size of 1.5–3.5 mg under air at a heating rate of 10 °C/min up to 800 °C from ambient temperature. The concentration of RB 4 (residual) in the synthetic dye effluent was spectrophotometrically estimated by measuring the absorbance at 573 nm using UV–visible absorption spectrometer (Perkin Elmer Lambda 35). The RB 4 dye concentration in the dyed cotton fabrics was spectrophotometrically estimated by measuring the absorbance at 601 nm using Gretag Macbeth spectrophotometer. Scanning Electron Microscopic (SEM) studies of SAP, DNP and RB 4 adsorbed DNP-16 at different magnifications were recorded using ZEISS EVO Series SEM model EVO 50. The equilibrium swelled and lyophilized DNP and SAP samples were used for recording SEM micrographs.

2.6. Swelling studies

The degree of swelling of DNP in water was measured in double distilled water using a tea bag as discussed elsewhere (Dhanapal et al., 2013) by taking 0.1 g of sieved sample in 200 mL of distilled water at 30 °C under equilibrium swelling conditions (4 h). The swelling profiles were constructed by plotting the water-absorbed during various time intervals at 30 °C against time. The equilibrium swelling (ES) was calculated by taking an average of three absorption measurements using Eq. (1):

$$ES = \frac{W_s - W_d}{W_d} \quad (1)$$

where W_s and W_d are the weights of the swollen gel and the dry sample, respectively.

2.7. Measurement of mechanical properties

The mechanical strength of the water swellen DNP-16 and SAP were measured at room temperature in terms of elastic modules and ultimate tensile strain using tensile-compressive tester (Tensilon RTC-1310A, Orientec Co.) and also by visual observation of the physical appearance of the samples under compression (Fig. 4). These tests were performed using swellen cylindrical gel samples of 10 mm diameter and 5 mm thickness. DNP-16 and SAP samples were kept on the platform of the compressor and a progressive load was applied through the upper plate of the compressor till the onset of damage, and this is measured as ultimate compressive stress. Their corresponding ultimate compressive strain and moduli values were also measured. The strain under compression is defined as the change in the thickness relative to the thickness of the specimen. For the tensile tests of DNP-16 and SAP samples were stretched parallel to the sample axis using a clamp attachment at a strain rate of 10%/min. Strain rates were referenced to the initial thickness of length of specimen. Failure points of compressive and tensile tests were determined from the peak of the stress–strain curve.

2.8. Dying using virgin and recovered dye

3.7 g of well scoured, accurately weighed, bleached and wetted cotton fabric was dipped in the dyebath (2% RB 4 cold brand dye solution, material: liquor ratio as 1:20) for 10 min. Then 2.3 g of NaCl as dye exhausting agent was added in two installments and the dyebath was set aside for another 20 min. Then 0.5 g of Na_2CO_3 was added as dye fixing agent to the dyebath and allowed for dye fixation for another 60 min (Tarun & Gobi, 2012). The unfixed dye in the fabric was removed by cold and hot water rinsing followed by detergent washing. The dyed fabric was air dried and its visible absorbance was measured. These fabric washings with water were added into the dye bath solution. The unfixed dye in the dyebath solution after dying was recovered by passing through DNP-16 in a column using isopropanol eluent and the dye was recovered by distilling out isopropanol. The adsorbed RB 4 on DNP-16 was desorbed via Soxhlet extraction using isopropanol as solvent over a period of 24 h. The adsorption–desorption of RB 4 was performed over five times for the same adsorbent to determine the frequency of reusability of the DNP in the effluent treatment. After each cycles of adsorption–desorption, DNP-16 was washed with distilled water thrice and then dried in an air oven at 60 °C for reuse. The amount of RB 4 in the dye solution was quantified. Recovered RB 4 dyebath was also prepared with same concentration by adopting aforesaid method, and the solid state absorption spectra were recorded and compared with virgin dyed specimen. The color fastness properties of the dyed fabric were also determined over a period of 12 h under sunlight and in soap solution to record and compare the absorption spectra (Fig. 2(b)).

2.9. Column mode adsorption studies

Adsorption experiments were performed in a glass column (Vijaya, Popuri, Boddu, & Krishnaiah, 2008) of 1 cm diameter and 80 cm length. The column was filled with 10 g of powdered and sieved adsorbent without voids. 100 mL of RB 4 dye solution (1, 2, 3, 4 and 5×10^3 mg/L) was added to the column at 30 °C. The effluent solution was collected at various time intervals after 30 min retention time within the column and the concentration of dye in solution was estimated spectrophotometrically at 573 nm. An average of triplicate was used for the dye concentration. The equilibrium

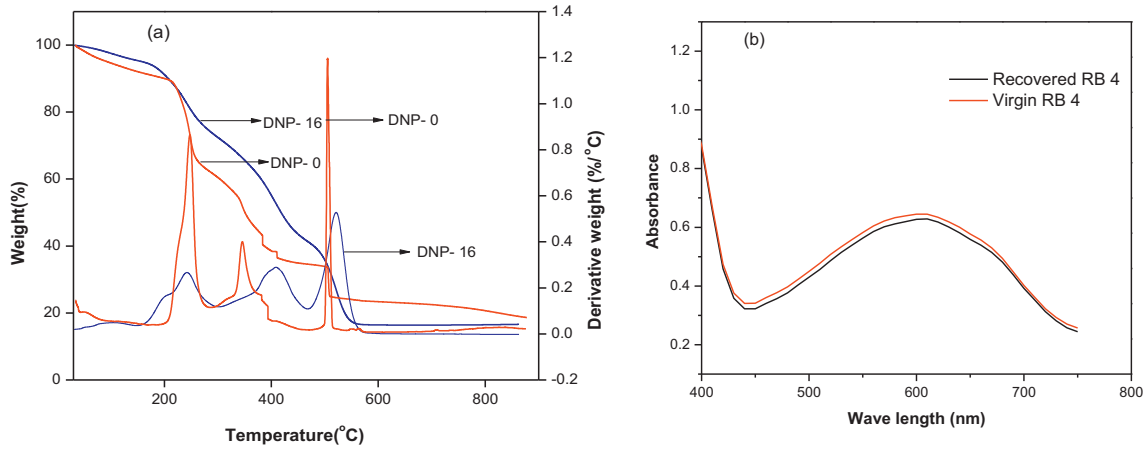

Fig. 2. TG/DTG traces of (a) DNP-0 and DNP-16, and visible absorption spectra of virgin and recovered dyed specimen (b).

adsorption of RB 4 was calculated using the mass balance equation (2):

$$q_e = (C_i - C_e)\frac{V}{W}(\text{mg/g}) \quad (2)$$

where q_e is the equilibrium amount of dye adsorbed (mg/g) onto the adsorbents (q_e is the average value of three experiments). C_i the initial concentration of dye in the dye effluent (mg/L), C_e is the equilibrium concentration of the dye in solution (mg/L), V is the volume of the solution (L) and W is the weight of the adsorbent (g).

2.10. Adsorption isotherm modeling

Equilibrium isotherms for adsorption are fundamental in describing the interactive behavior between solutes and adsorbents, and are important in the selection of adsorbent for a solute. The equilibrium relationship between an adsorbate and adsorbent can be described using isotherm models (Uma, Banerjee, & Sharma, 2013). In the present investigation the dye adsorption data are analysed by fitting in Langmuir and Freundlich models as per Eqs. (3) and (4), respectively.

$$\frac{1}{q_e} = \frac{1}{q_m} + \frac{1}{q_m K_L C_e} \quad (3)$$

$$\log q_e = \log K_F + N \log C_e \quad (4)$$

where q_m is the equilibrium monolayer adsorption capacity (mg/g) is a measure of dye uptake and K_L is the Langmuir constant (L/mg) will imply the adsorption energy, K_F is the Freundlich constant, which predicts the quantity of dye adsorbed (mg/g) per gram of polymer under equilibrium, N is the measure of the nature and strength of the adsorption process and of the distribution of active sites.

2.11. Adsorption kinetics

The kinetic of RB 4 adsorption was tested using pseudo-first and second order kinetic models based on Eqs. (Uma et al., 2013) (5) and (6), respectively.

$$\log(q_e - q_t) = \log q_e - \left(\frac{k_1}{2.303}\right) t \quad (5)$$

$$\frac{dq_t}{d_t} = k_2(q_e - q_t)^2 \quad (6)$$

where q_e and q_t (both in mg/g) are amounts of RB 4 adsorbed at equilibrium and at time 't' respectively, k_1(min^{-1}) and k_2 (g mg^{-1} min^{-1}) are the rate constant of pseudo-first and second order kinetics, respectively.

2.12. Thermodynamics of adsorption

The changes in the thermodynamic parameters for the adsorption process namely Gibbs free energy (ΔG°), enthalpy (ΔH°) and entropy (ΔS°) for RB 4 dye adsorption were determined (Bhattacharyya & Gupta, 2007) using Eq. (7):

$$\ln K_d = \frac{\Delta S^\circ}{R} - \frac{\Delta H^\circ}{RT} \quad (7)$$

where K_d is the distribution coefficient of the adsorbate ($K_d = C_e/q_e$), R is the universal gas constant (8.314 J K^{-1} mol^{-1}), T is the absolute temperature (K). The plot of ln K_d as a function of $1/T$ yields a straight line. From its slope and intercept the average values of ΔH° and ΔS°, respectively were obtained for the temperature range 303–323 K.

3. Result and discussion

3.1. Mechanism of crosslinking

The Ca^{2+} ionic crosslinking in NaAlg which occurs through (Lee & Mooneya, 2012) the α-L-guluronate (G-blocks) of NaAlg and the possible mechanism for photo crosslinking between ionically crosslinked NaAlg and SAP are presented in Scheme 1. During irradiation of the SAP and ionic crosslinked NaAlg blend, carbon centered radicals may be formed by the preferential homolytic scission of C—H bond in methine carbon (Decker, 1984). This may facilitate crosslinking via radical coupling (Scheme 1). Moreover during irradiation oxygen insertion reaction may also occur between the methine carbon and hydrogen () leading to the formation of hydroperoxide (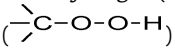) weak links. Since this link which is photolabile may result in the formation of oxygen centered radicals  and H—O• during photolysis these may also induce crosslinking (Scheme 1).

3.2. FT-IR analysis

Typical FT-IR spectra of SAP, NaAlg and DNP-16, RB 4 adsorbed DNP-16 and DNP-0 are displayed in Fig. 1(b). Analysis of these IR spectra (Nuran, Kursun, & Inal, 2010; Pawar & Edgar, 2012; Solpan, Torun, & Guven, 2008) indicated the presence of SAP and NaAlg moieties in the photo crosslinked double network polymer. For example, the absorption peaks at 1730 and 1547 cm^{-1} attributed to the >C=O stretching of ester group (TMPTA) and carboxylate anion (KA), respectively (Dhanapal et al., 2013) present in SAP were also present in DNP. The peak at 1655 cm^{-1} indicated the presence

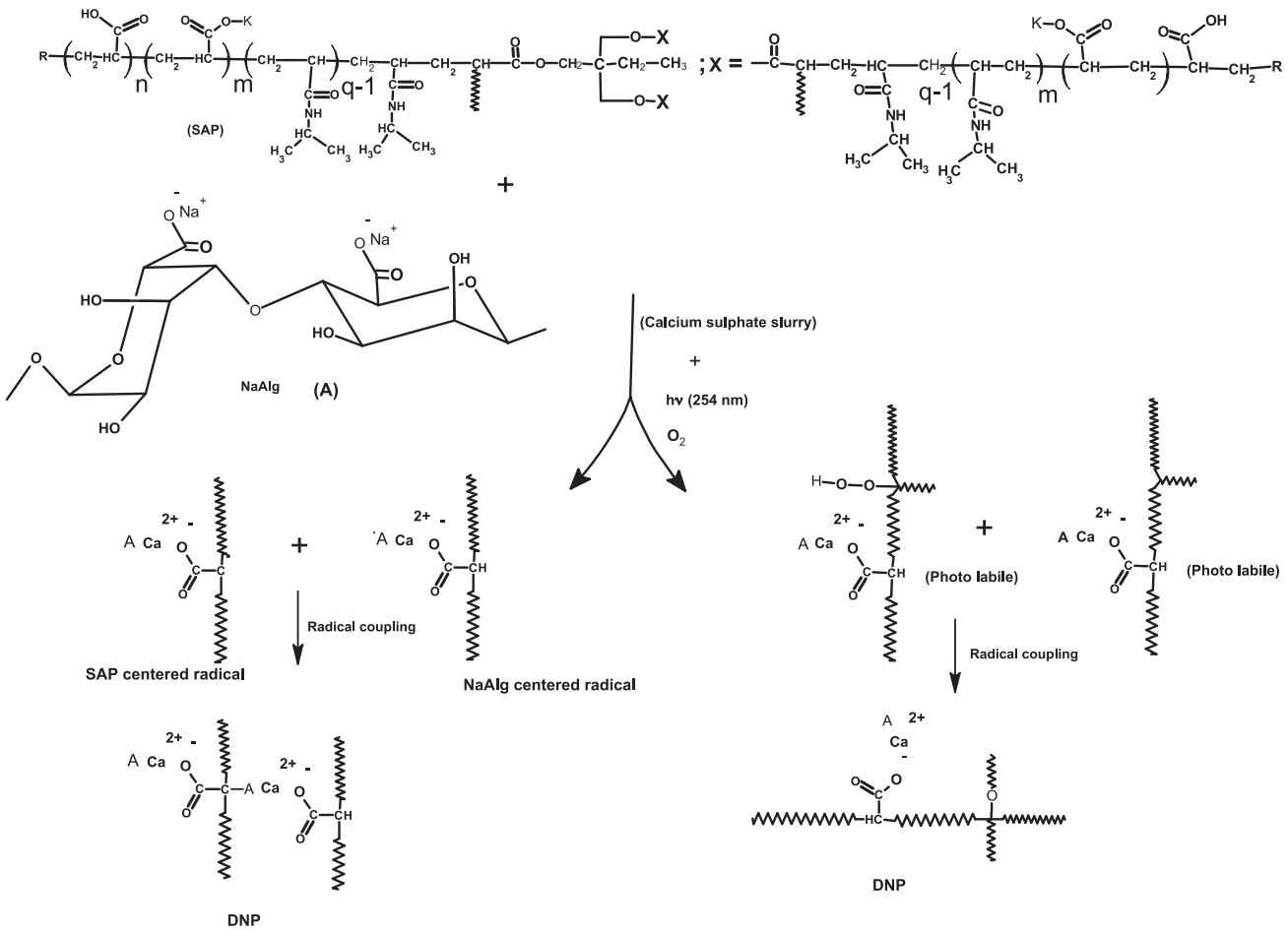

Scheme 1. Photo crosslinking mechanism between SAP and NaAlg.

of NIPAAm residue in SAP moiety. The IR spectra also showed a broad peak at 3502 cm^{-1}(—OH), a peak at 1612 cm^{-1} is endorsed to —COO^-, and a peak at 1029 cm^{-1} corresponding to C—O group are characteristics of the polysaccharides (NaAlg). The characteristic peak of calcium alginate appeared at 810–813 cm^{-1} (—Ca—O) in DNP-16 and DNP-0. Representative IR spectra of virgin and desorbed RB 4 are given in Fig. 1(c). The broad peaks at 3450 and 3458 cm^{-1} are attributed to the amino groups of virgin and desorbed RB 4, respectively. Peaks at 1720 and 1639 cm^{-1} indicated the presence of exocyclic >C=O and endo cyclic >C=N groups in the dye. The characteristic peaks at 1140 and 674 cm^{-1} correspond to >C—N and >C—Cl groups of dye.

3.3. TG analysis

TG thermograms for representative DNP samples (DNP-16 and DNP-0 (physical blend of NaAlg and SAP before irradiation)) are depicted in Fig. 2(a) showed multistep degradations. The initial weight loss up to 100 °C was attributed to the residual volatile matters such as moisture present in the SAP. The initial onset degradation of DNP at a temperature around 225 °C with considerable decomposition was ascribed to a complex process including dehydration of the saccharide rings, de-polymerization with the formation of water, CO_2 and methane (Wang & Wang, 2010). The degradation step above 300 °C is more likely due to the degradation initiated via the olefinic bonds, decarboxylation of carboxylate anion and scission of crosslinks, etc. The major degradation of DNP around 400 °C corresponding to a weight loss of 50% was more likely attributed to the degradation of SAP moiety. Comparison of DTG curves revealed that the thermal stability of the photo crosslinked double network is greater than that of the physical mixture.

3.4. Water uptake and dye adsorption

Water and dye uptake, and release profiles with respect to time for DNP-16 and DNP-0 are given in Fig. 3(a). The maximum equilibrium water uptake by DNP-16 and DNP-0 were 810 g/g and 698 g/g, respectively. The adsorption capacity of RB 4 on DNP-16 and SAP were 439 mg/g and 321 mg/g, respectively. Analysis of the adsorption profiles in Fig. 3(a) revealed that the water and dye uptake rates were greater than the corresponding release rates. The decrease in the release rates of water and dye may be due to the enhanced physico-chemical crosslinking through H-bonding with dye molecule (Dhanapal et al., 2013). However, in the absence of salts the adsorption capacity of DNP-16 was 545 mg/g (in the absence of co-ions). But at higher salt loading (ionic strength = >0.2062 mol/dm^3) during dying the adsorption capacity decreased to 245 mg/g. The possible reason for low adsorption capacity at high ionic strength is due to the screening of electrostatic interaction of opposite charges by the salt on the adsorbent surface.

3.5. Adsorption isotherms

The adsorption data of RB 4 on DNP-16 was fitted to Langmuir and Freundlich isotherms and the best fit for the adsorption of RB 4 on DNP-16 was found to be Langmuir based on the correlation coefficients (R^2) of Langmuir and Freundlich isotherms which

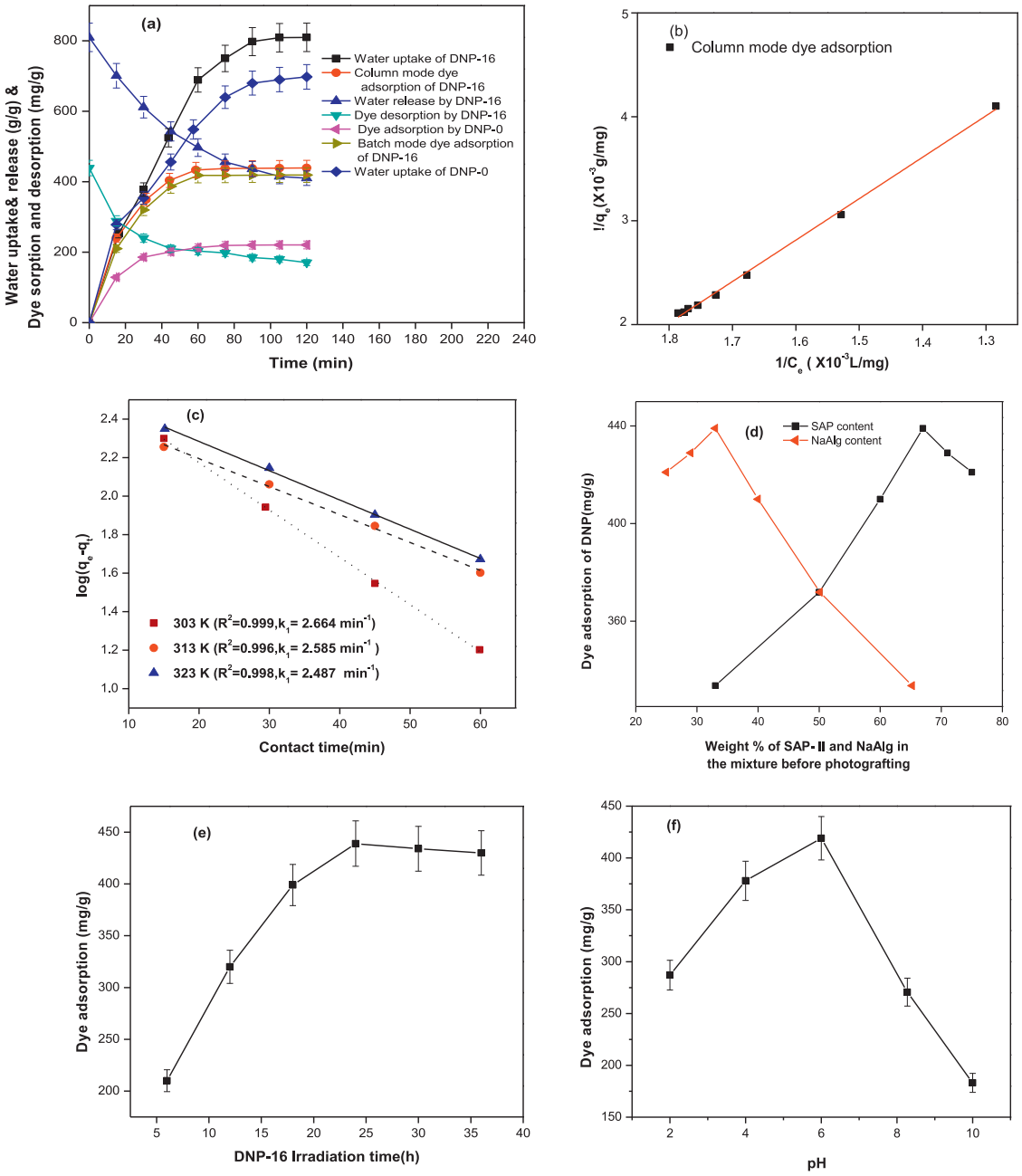

Fig. 3. Water and RB 4 uptake and their release profiles (a), Langmuir adsorption isotherm (b), pseudo-first-order adsorption kinetic model (c) at different temperatures, effect of weight % of SAP and NaAlg (d), irradiation time (e), and pH (f) on dye adsorption.

also indicated monolayer dye adsorption (Uma et al., 2013). Langmuir isotherm parameters q_m and K_L were calculated from the slope and intercept of the plot $1/q_e$ vs. $1/C_e$ (Fig. 3(b)) and these parameters are given in Table 1. The K_L which is essentially an equilibrium constant, and its variation of with temperature can be used to estimate the enthalpy change accompanying adsorption, affinity between the adsorbent and adsorbate. The value q_m is comparable to the adsorption capacities of some other

Table 1
Langmuir and Freundlich adsorption isotherm parameters for DNP-16 and RB 4 system.

Sample code	Adsorption isotherm parameters			
DNP-16[a]	Langmuir	q_m (mg/g)	K_L (L/mg)	R^2
		446	1.283	0.999
	Freundlich	K_F (mg/g)	N	R^2
		2.119	0.825	0.919

[a] DNP-16 was prepared by keeping weight % of SAP: weight % of NaAlg in mixture as 67:33. For the SAP synthesis [AA] and [KPS] were 1.2 M and 0.00 M, respectively, and volume of experimental solution was 40 mL.
SAP (S/A = 0.55, TMPTA = 0.002 M and NIPAAm = 0.05 M), S/A = [Potassium acrylate]/[AA].

Table 2
Pseudo-first- and second-order adsorption kinetic parameters for DNP-16 and RB 4 system at different temperatures.

Sample code	Kinetic model	T (K)	Parameters (q_e = mg/g, k_1 = min^{-1} and k_2 = g mg^{-1} min^{-1})	R^2
DNP-16	Pseudo-first order	303	q_e = 439 k_1 = 4.2	0.998
		313	q_e = 304 k_1 = 1.69	0.999
		323	q_e = 282 k_1 = 1.31	0.998
	Pseudo-second order	303	q_e = 77.23 k_2 = 5.23	0.977
		313	q_e = 42.12 k_2 = 4.65	0.974
		323	q_e = 31.72 k_2 = 4.50	0.987

adsorbent materials for RB 4. These figures indicate that the DNP-16 is a good adsorbent for recycling of the textile dye from effluent. This was also supported by the nearly identical values for the experimentally determined equilibrium dye adsorption and theoretically calculated Langmuir equilibrium RB 4 adsorption isotherm parameters.

3.6. Adsorption kinetics

The rate of adsorption an important parameter is essential for column design and process optimization for successful commercial applications such as heavy metal removal and dye adsorption from effluent. Comparing the adsorption capacities (mg/g) of DNP-16 and DNP-0 for RB 4 measured as a function of time (Fig. 3(a)) revealed rapid dye adsorption during the initial 60 min of contact time, which subsequently slowed down over a longer period of time until the equilibrium was attained. During the initial 60 min contact time, 78% of equilibrium adsorption for DNP-16 was accounted. The rapid dye adsorption (Uma et al., 2013) is the most probably due to the abundant availability of active sites on the adsorbent, whereas with the gradual occupancy of these sites, adsorption became less efficient after 60 min of contact time. The degree of dye adsorption was tested with the pseudo-first order and pseudo-second order kinetic models (parameters are given in Table 2) and the best fit kinetic model was found to be pseudo-first order by comparing the R^2 values of the plots '$\log(q_e - q_t)$ vs. t' (Fig. 3(c)) and t/q_t vs. t for pseudo-first order and pseudo-second order kinetic models, respectively (Uma et al., 2013). The rate constants of adsorption determined from the slopes of profiles in Fig. 3(c) were decreased with temperature, indicating enhanced temperature does not favor the adsorption of RB 4. The extent of dye adsorption, and the amount of dye adsorbed per unit mass of the adsorbents (q_e) decreased appreciably with temperature which may be attributed to the competing desorption process at enhanced temperatures.

3.7. Thermodynamics of dye adsorption

The ΔG°, ΔH° and ΔS° values for dye adsorption were measured as per Eq. (7). The negative values of ΔG° namely, $-618\ kJ\ mol^{-1}$, $-1610\ kJ\ mol^{-1}$ and $-2263\ kJ\ mol^{-1}$ for the temperature 303 K, 313 K and 323 K, respectively, indicated that the RB 4 adsorption on DNP was spontaneous. The average negative value of ΔH° ($-2922\ kJ\ mol^{-1}$) for the above temperatures indicated that adsorption is exothermic which may be due to the weak interactions between the adsorbent and dye. The positive value of entropy ($9.98\ kJ\ mol^{-1}$) was attributed to the increased volume of the system (adsorbent and dye solution) through swelling which may enhance the mobility of the adsorbed dye molecule. The abovediscussed observations indicated that the DNP-16 is a good candidature material for dye removal (Olgun & Atar, 2012) from the textile dye effluent.

3.8. Water and dye release studies

The mechanism of water and dye released from swelled and dye adsorbed DNP-16 was analyzed using the power law (Dhanapal et al., 2013) Eq. (8)

$$\frac{M_t}{M\infty} = kt^n \tag{8}$$

where M_t is the amount of the water/dye released by the swellen polymer at time t, M_∞ the amount of the water/dye released after infinite time, k the constant and n the diffusion exponent.

The values of diffusion exponents (n) were found to be in the range of 0.3–0.38 and 0.39–0.43 for water and dye solutions, respectively. This implied that the release mechanism appeared to be non-Fickian.

3.9. SEM

The surface morphological features of the freeze-dried SAP and DNP-16, and DNP-0 after swelling in water and dye solution was analyzed by SEM and the representative SEM micrographs are shown in Fig. 4. Analysis of these SEM images revealed the formation of pores during freeze drying and porous network structure (Fig. 4(a and b)) in irradiated samples. The porous morphology is more likely due to water evaporation. The shapes of the pores are irregular and interconnected. The massive distribution of pores in the freeze-dried samples indicated water uptake throughout the material and the presence of void volume. The unequal pore sizes may imply that the crosslinking may not be uniform throughout the material. The porous structure appeared to be more compact in DNP-16 than in SAP Fig. 4(a and d) perhaps due to intermolecular crosslinking. These pores may be the areas, where the water permeation occurs and interaction sites are available to form secondary bonds with dyes, metal ions, drugs, etc. (Attaa, Abdel-Rahman, Aassy, Ahmed, & Hamza, 2011; Pourjavadi, Jahromi, Seidi, & Salimi, 2010). Analysis of Fig. 4(c) also confirms the adsorption of RB 4 on DNP-16. Hence, the porous structure appeared to be the predominant cause for the high swellability and dye adsorption. The porosity and network structure revealed by SEM micrographs corroborated a three-dimensional structure for DNP.

3.10. Mechanical properties

The physico-chemical crosslinked SAP shatters into pieces under modest compression (Fig. 5(c and e)) due to its brittleness nature. But the photo crosslinked DNP was able to withstand cycles of compression and regains its original shape on relieving

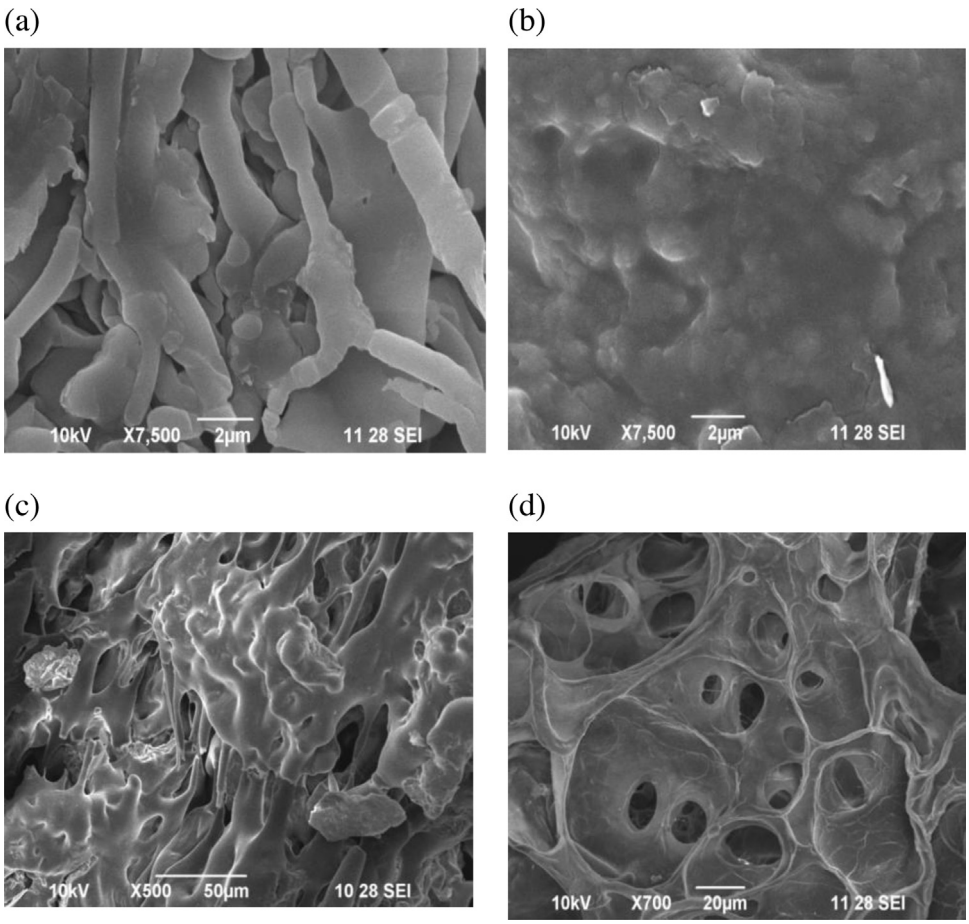

Fig. 4. SEM micrographs of equilibrium swelled, lyophilized and freeze dried DNP-16 (a), DNP-0 (b), DNP-16 (c, RB 4 adsorbed) and SAP (d).

the compression and this is displayed in Fig. 5(b, d and f). Moreover, the crosslinked DNP can able to hold water and water soluble material through adsorption even under compression unlike SAP. This demonstrated that DNP was having significantly improved mechanical properties in terms of elongation and modulus. Fig. 5(a) shows typical compressive stress–strain curve of DNP-16 and SAP. The representative DNP-16 gel showed a compressive elastic modulus 750 MPa, which is very much greater than that of SAP (73 MPa). The ultimate stress and the strain at the breaking (failure) point of DNP-16 and SAP were 36.4 MPa (at% elongation 354) and 3.54 MPa (at% elongation 3.5), respectively. Hence the adsorbent may be persistently used for textile effluent treatment process.

3.11. Reusability of recycled dye and adsorbent

The most important requirement for the adsorbent is its reusability even after several adsorption–desorption cycle. This was tested by the constancy of its adsorbent capacity during the repeated cycle of it usage. It was observed that the initial adsorption capacity of DNP-16 for RB 4 was 439 mg/g. The adsorption capacity remains nearly constant after five adsorption–desorption cycle demonstrating that DNP-16 may be repeatedly used for the removal of dye from dye effluent in commercial effluent treatment plants due to the improved mechanical properties of DNP-16 over SAP. Moreover, the molar extinction coefficients values at 573 nm (λ_{max}) for the virgin (865,520 L/mol cm) and recovered dye (865,531 L/mol cm) were nearly identical supporting the original chemical nature of the recovered dye. Besides, IR spectra of virgin RB 4 and desorbed RB 4 were identical even after five adsorption–desorption cycles demonstrating that the dye remained stable structurally and hence the recovered RB 4 may be reused for dying fabrics. The solid state visible absorption spectra of cloth dyed using virgin and recovered dye (Fig. 2(b)) were nearly identical corroborating the chemical stability of the dye during dye recovery processes in column mode. The constant color fastness properties of the dyed fabric with RB 4 and recovered RB 4 indicated that the chemical nature of recovered dye remained same, and the dyed fabrics showed good color fastness under sunlight and in soap solution.

3.12. Factors affecting dye adsorption

3.12.1. DNP composition

The quantum of dye adsorption by DNP was analyzed as a function of its composition from the profile (Fig. 3(d)) constructed by plotting weight percentage of SAP and NaAlg in the blend vs. amount of dye adsorbed. As the % of NaAlg increases there is an increase in the dye uptake initially and with the further increase in NaAlg content the dye uptake decreased. DNP with increased % of SAP displayed an initial increase in dye uptake which then decreased for enhanced % of SAP. The observations on the extend of dye adsorption as a function of DNP composition could be attributed to the poor crosslinking due to increased viscosity of the medium, variation in photo crosslinking, physico-chemical crosslinking and electrostatic repulsion between carboxylate anions as well.

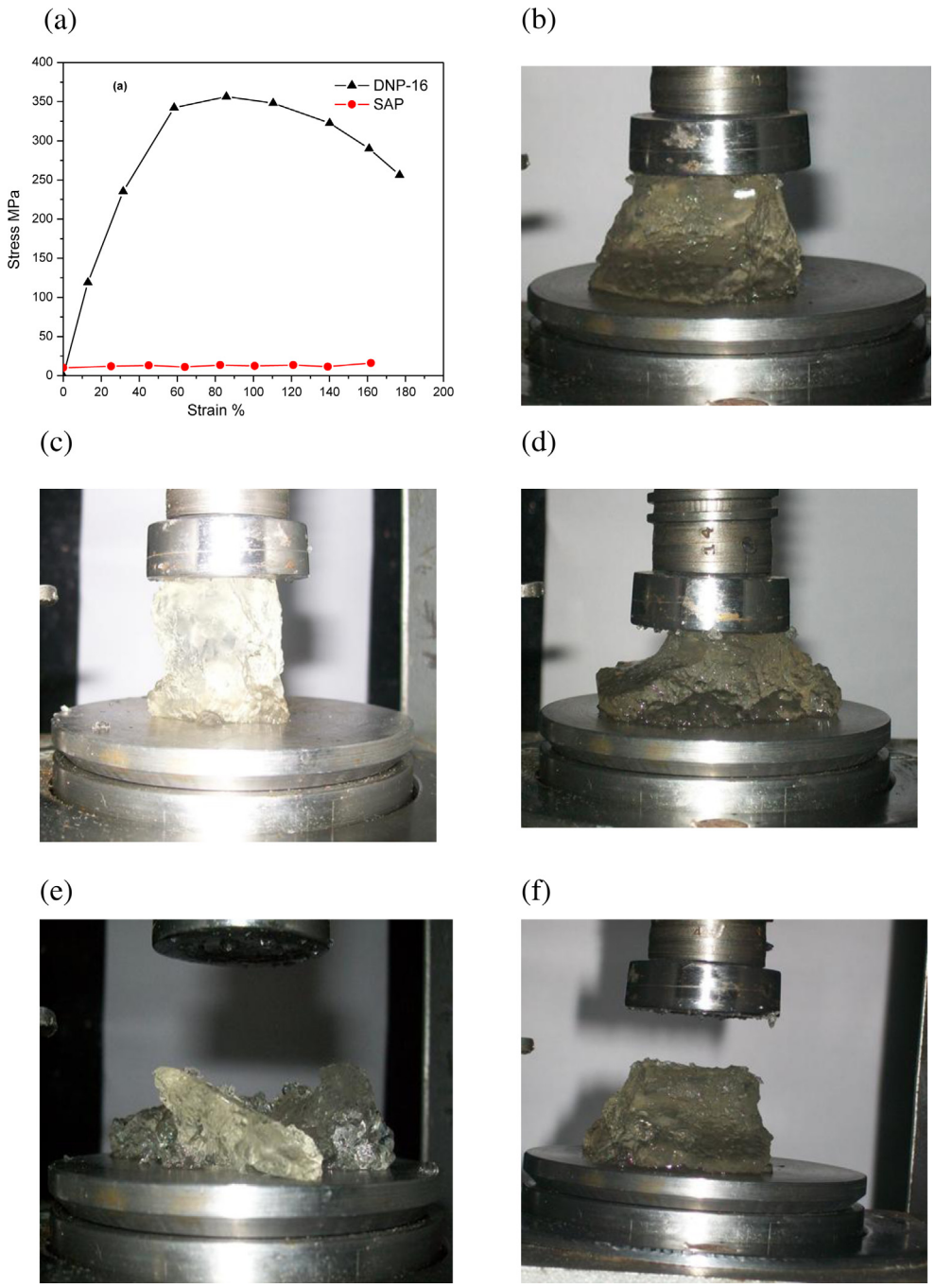

Fig. 5. Stress–strain curve (a) for DNP-16 and SAP, photographs of DNP-16 with 90% water content before compression (b), during compression (d), after compression (f), SAP before compression (c) and after compression (e).

3.12.2. Irradiation time

Duration of irradiation has also affected the dye adsorption on DNP for a given composition and adsorption vs. irradiation time curve for a representative DNP-16 is shown in Fig. 3(e). The DNP-16 (24 h irradiated) had absorbed 810 g/g of water under ambient conditions. However, it had adsorbed 478 mg/g of dye in distilled water. For irradiation time greater than 24 h both water uptake and dye adsorption were reduced (30 h), and this may be attributed to extensive crosslinking.

3.12.3. pH values

The pH of dye effluent is one of the major factors affecting the dye adsorption behavior of an adsorbent and the effect of pH on adsorption of RB 4 on DNP-16 over a pH range of 2–10 are given in Fig. 3(f). The functional groups on the surface of an adsorbent may be altered by the variation in pH of dye effluent taken for treatment process. It was obvious that the adsorption capacity increased with increasing pH of dye effluent, and significant enhancement was observed till it reached a pH of 6. Further increase of pH beyond 8 has reduced the dye adsorption due to the electrostatic repulsive force between adsorbent and adsorbate. At acidic pH, most of the carboxyl groups on the surface of the adsorbent exist in the form of —COOH, which lead to a competition between hydrogen ion and the cationic RB 4 to seek active site on adsorbent. This may result in the reduction of dye adsorption. At pH 6, the adsorption capacities increased hardly owing to the

buffer action of —COOH and —COO^- groups (Liu, Zheng, & Wang, 2011).

4. Conclusions

DNP of different compositions were synthesized through photochemical crosslinking of NaAlg and SAP at 254 nm. TG analysis and the mechanical properties of DNP revealed that, it is sufficiently thermally stable in air and can withstand usual environmental conditions. SEM micrographs of swelled, freeze dried and lyophilized DNP-16 revealed network formation and RB 4 adsorption. The nearly identical visible absorption spectra of the dyed fabrics for virgin and recovered RB 4, and the constant color fastness properties of the dyed fabric with these dyes indicated that the chemical nature of recovered dye remained same. DNP was evaluated as an adsorbent in column mode for textile effluent treatment taking RB 4 as a typical reactive dye, and the adsorption capacity of DNP-16 was 439 mg/g. In every adsorption–desorption cycle almost constant amount of dye was recovered. The equilibrium dye adsorption profile at different concentrations of dye implied predominantly Langmuir adsorption isotherm. The kinetics data of adsorption corroborated pseudo-first order model. The dye adsorption–desorption followed a non-Fickian mechanism. Evaluation of changes in thermodynamic parameters such as ΔG°, ΔH° and ΔS° for dye adsorption indicated that adsorption is spontaneous and exothermic for the chosen double network polymer. This study demonstrated that DNP-16 can serve as a potential adsorbent for the effective recycling of dyes from the textile effluent in commercial effluent treatment plants.

Acknowledgment

The authors thank the management of Bannari Amman Institute of Technology, Sathyamangalam for encouraging research work by extending the required facilities.

References

Attaa, A. M., Abdel-Rahman, A. A.-H., Aassy, I. E. El, Ahmed, F. Y., & Hamza, M. F. (2011). Adsorption properties of uranium(VI) ions on reactive crosslinked acrylamidoxime and acrylic acid copolymer resins. *Journal of Dispersion Science and Technology*, *32*, 84–94.

Baskaralingam, P., Pulikesi, M., Ramamurthi, V., & Sivanesan, S. (2006). Equilibrium studies for the adsorption of acid dye onto modified hectorite. *Journal of Hazardous Materials*, *136*, 989–992.

Bhattacharyya, K. G., & Gupta, S. S. (2007). Adsorptive accumulation of Cd(II), Co(II), Cu(II), Pb(II), and Ni(II) from water on montmorillonite: Influence of acid activation. *Journal of Colloid and Interface Science*, *310*, 411–424.

Decker, C. (1984). Degradation of poly(vinyl chloride) by U.V. radiation – II. *European Polymer Journal*, *20*, 149–155.

Dhanapal, V., Vijayakumar, V., & Subramanian, K. (2013). Synthesis and evaluation of trimethylolpropane triacrylate crosslinked superabsorbent polymers for conserving water and fertilizers. *Journal of Applied Polymer Science*, *129*, 1350–1361.

Dhodapkar, R., Rao, N. N., Pande, S. P., & Kaul, S. N. (2006). Removal of basic dyes from aqueous medium using a novel polymer: Jalshakti. *Bioresource Technology*, *97*, 877–885.

Gong, J. P., Katsuyama, Y., Kurokawa, T., & Osada, Y. (2003). Double-network hydrogels with extremely high mechanical strength. *Advanced Materials*, *15*, 1155–1158.

Guilherme, M. R., Reis, A. V., Takahashi, S. H., Rubira, A. F., Feitosa, J. P. A., & Muniz, E. C. (2005). Synthesis of a novel superabsorbent hydrogel by copolymerization of acrylamide and cashew gum modified with glycidyl methacrylate. *Carbohydrate Polymers*, *61*, 464–471.

Kadirvelu, K., Brasquet, C., & Cloiree, P. (2000). Removal of Cu(II), Pb(II) and Ni(II) by adsorption on to activated carbon cloths. *Langmuir*, *16*, 8404–8409.

Kobaslija, M., & McQuade, D. T. (2006). Removable colored coatings based on calcium alginate hydrogels. *Biomacromolecules*, *7*, 2357–2361.

Lee, K. Y., & Mooneya, D. J. (2012). Alginate: Properties and biomedical applications. *Progress in Polymer Science*, *37*, 106–126.

Liu, Y., Zheng, Y., & Wang, A. (2011). Effect of biotite content of hydrogels on enhanced removal of methylene blue from aqueous solution. *Ionics*, *17*, 535–543.

Marandi, G. B., Sharifnia, N., & Hosseinzadeh, H. (2006). Synthesis of an alginate–poly(sodium acrylate-coacrylamide) superabsorbent hydrogel with low salt sensitivity and high pH sensitivity. *Journal of Applied Polymer Science*, *101*, 2927–2937.

Nakajima, T., Furukawa, H., Tanaka, Y., Kurokawa, T., Osada, Y., & Gong, J. P. (2009). True chemical structure of double network hydrogels. *Macromolecules*, *42*, 2184–2189.

Nasr, M. F., Abo El-Ola, S. M., Ramadan, A., & Hashem, A. (2006). A comparative study between the adsorption behavior of activated carbon fiber and modified alginate I. Basic dyes adsorption. *Polymer-Plastics Technology and Engineering*, *45*, 335–340.

Nuran, I., Kursun, F., & Inal, M. (2010). Graft copolymerization of itaconic acid onto sodium alginate using benzoyl peroxide. *Carbohydrate Polymers*, *79*, 665–672.

Olgun, A., & Atar, N. (2012). Equilibrium, thermodynamic and kinetic studies for the adsorption of lead(II) and nickel(II) onto clay mixture containing boron impurity. *Journal of Industrial and Engineering Chemistry*, *18*, 1751–1757.

Orthman, J., Zhu, H. Y., & Lu, G. Q. (2003). Use of anion clay hydrotalcite to remove colored organics from aqueous solutions. *Separation and Purification Technology*, *31*, 53–59.

Paulino, A. T., Guilherme, M. R., Reis, A. V., Campese, G. M., Muniz, E. C., & Nozaki, J. (2006). Removal of methylene blue dye from an aqueous media using superabsorbent hydrogel supported on modified polysaccharide. *Journal of Colloid and Interface Science*, *301*, 55–62.

Pawar, S. N., & Edgar, K. J. (2012). Alginate derivatization: A review of chemistry, properties and applications. *Biomaterials*, *33*, 3279–3305.

Pourjavadi, A., Jahromi, P. E., Seidi, F., & Salimi, H. (2010). Synthesis and swelling behavior of acrylated starch-g-poly(acrylic acid) and acrylated starch-g-poly(acrylamide) hydrogels. *Carbohydrate Polymers*, *79*, 933–940.

Rajeswari, S., Namasivayam, C., & Kadirvelu, K. (2001). Orange peel as an adsorbent in the removal of acid violet 17(acid dye) from aqueous solution. *Waste Management*, *21*, 105–110.

Solpan, D., Torun, M., & Guven, O. (2008). The usability of (sodium alginate/acrylamide) semi-interpenetrating polymer networks on removal of some textile dyes. *Journal of Applied Polymer Science*, *108*, 3787–3795.

Tahir, S. S., & Rauf, N. (2006). Removal of a cationic dye from aqueous solutions by adsorption onto bentonite clay. *Chemosphere*, *63*, 1842–1848.

Tarun, K., & Gobi, N. (2012). Calcium alginate/PVA blended nano fibre matrix for wound dressing. *Indian Journal of Fibre and Textile Research*, *37*, 127–132.

Tsai, W. T., Chang, C. Y., Ing, C. H., & Chang, C. F. J. (2004). Adsorption of acid dyes from aqueous solution on activated bleaching earth. *Journal of Colloid and Interface Science*, *275*, 72–78.

Uma, Banerjee, S., & Sharma, Y. C. (2013). Equilibrium and kinetic studies for removal of malachite green from aqueous solution by a low cost activated carbon. *Journal of Industrial and Engineering Chemistry*, *19*, 1099–1105.

Vijaya, Y., Popuri, S. R., Boddu, V. M., & Krishnaiah, A. (2008). Modified chitosan and calcium alginate biopolymer sorbents for removal of nickel(II) through adsorption. *Carbohydrate Polymers*, *72*, 261–271.

Wang, J. J., & Liu, F. (2013). Enhanced adsorption of heavy metal ions onto simultaneous interpenetrating polymer network hydrogels synthesized by UV irradiation. *Polymer Bulletin*, *70*, 1415–1430.

Wang, W., & Wang, A. (2010). Synthesis and swelling properties of pH-sensitive semi-IPN superabsorbent hydrogels based on sodium alginate-g-poly(sodium acrylate) and polyvinyl pyrrolidone. *Carbohydrate Polymers*, *80*, 1028–1036.

Yasuda, K., Gong, J. P., Katsuyama, Y., Nakayama, A., Tanabe, Y., Kondo, E., et al. (2005). Biomechanical properties of high-toughness double network hydrogels. *Biomaterials*, *26*, 4468–4475.

Zheng, Y., Huang, D., & Wang, A. (2011). Chitosan-g-poly(acrylic acid) hydrogel with crosslinked polymeric networks for Ni^{2+} recovery. *Analytica Chimica Acta*, *687*, 193–200.